PHOTOSYNTHETICA
International Journal for Photosynthesis Research

DOI 10.32615/ps.2023.041 PHOTOSYNTHETICA 61 (SI): 465-472, 2023

Special issue in honor of Prof. Győző Garab

Photosynthetic reaction center/graphene bio-hybrid for low-power optoelectronics

J. VUJIN[*], T. SZABÓ[**], R. PANAJOTOVIC[*], A.G. VÉGH[***], L. RINYU[#], and L. NAGY[**,##,+]

Institute of Physics Belgrade, University of Belgrade, Pregrevica 118, 11080 Belgrade, Serbia[*]
Institute of Medical Physics and Informatics, University of Szeged, Korányi Fasor 9, H-6720 Szeged, Hungary[**]
HUN-REN Biological Research Centre, Szeged, Institute of Biophysics, Temesvári Krt. 62, Szeged, Hungary[***]
Isotope Climatology and Environmental Research Centre (ICER), HUN-REN Institute for Nuclear Research, Bem tér 18/c, 4026 Debrecen, Hungary[#]
HUN-REN Biological Research Centre, Szeged, Institute of Plant Biology, Temesvári Krt. 62, Szeged, Hungary[##]

Abstract

Photosynthetic reaction center (pRC) purified from *Rhodobacter sphaeroides* 2.4.1 purple bacteria was deposited on a graphene carrier exfoliated from the liquid phase and layered on the surface of SiO_2/Si substrate for optoelectronic application. Light-induced changes in the drain-source current *vs*. gate voltage are demonstrated. Dried photosynthetic reaction centers/graphene composite on SiO_2/Si shows a photochemical/-physical activity, as a result of interaction with the current flow in the graphene carrier matrix. The current changes are sensitive to light, due to the contribution from the charge separation in the pRC, and to the applied gate and drain-source voltages.

Keywords: field effect; graphene; liquid-phase exfoliation; optoelectronics; photosynthetic reaction center.

Introduction

At the turn of the 21st century, the synergy of research laboratories of fundamental and applied sciences together with the emerging request for advanced technologies led to the constructive interference of a wide range of disciplines (such as optoelectronics, (bio)photonics, nanotechnology, and nanobionics). A new generation of optoelectronic systems designed for energy conversion, imaging devices, optical switches, and sensors (Tamiaki *et al.* 2006, Nagy *et al.* 2010, 2014; Giraldo *et al.* 2014, Szabó *et al.* 2015, Daliento *et al.* 2017) became valuable tools in modern science and industry (Nagy and Magyar 2022). In addition, discovering new types of nano(bio)hybrid materials provides the possibility to create functional complexes that are considered in the literature as materials for the future (Darder *et al.* 2007, Shoseyov and Levy 2008, Nagy *et al.* 2014, Szabó *et al.* 2015).

Highlights

- Interaction between electric current in graphene and charge transfer in pRCs
- Electric field effect on charge separation in photosynthetic reaction centers
- Photosynthetic reaction center/graphene biohybrid for low-power optoelectronics

Received 11 September 2023
Accepted 2 November 2023
Published online 10 November 2023

[+]Corresponding author
e-mail: lnagy@sol.cc.u-szeged.hu

Abbreviations: AFM – atomic force microscopy; CNT – carbon nanotube; CVD – chemical vapor deposition; CWDL – continuous wave diode laser; DI – de-ionized; I_{DS} – drain-source current; IR – infrared; LB – Langmuir–Blodgett; LBA – Langmuir–Blodgett assembly; LPE – liquid phase exfoliation; mRGO – mercapto reduced graphene oxide; pRC – photosynthetic reaction center; RMS – root mean square; SEM – scanning electron microscopy; U_{DS} – drain-source voltage; U_G – gate voltage; UV – ultraviolet.

Acknowledgements: The research was supported by the European Union and the State of Hungary, co-financed by the European Regional Development Fund in the project of GINOP-2.3.2.-15-2016-00009 'ICER'. Thanks are due to the Hungarian Ministry of Innovation and Technology, National Research, Development and Innovation Fund (OTKA grants FK-139067). The authors R.P. and J.V. acknowledge funding provided by the Institute of Physics Belgrade, through a grant by the Ministry of Education, Science, and Technological Development of the Republic of Serbia. Partial support was provided by the Eötvös Loránd Research Network (ELKH KÖ-36/2021).
Conflict of interest: The authors declare that they have no conflict of interest.

The new generation of technologies offers unique solutions for specific tasks, such as optimizing the size of the devices and sample quantity, aiming single-molecular, fast, reversible, online, real-time, remote operation, and highly reproducible, sensitive, selective responses (Magyar *et al.* 2013, 2016; Luka e*t al.* 2015, Szabó *et al.* 2017). There is a large number of reports and reviews summarizing the advantageous properties of graphene for a wide range of applications referring to its unique transport properties (optical and electric conductivity) (Geim and Novoselov 2007, Geim 2009) as well as its extraordinarily high mechanical (strength and flexibility) and chemical stability (Blake e*t al.* 2008, Wang *et al.* 2008, Kim *et al.* 2009, Li *et al.* 2009).

To utilize the full potential of graphene, the selection of the appropriate methods of synthesis plays an important role. In addition to commonly used preparation methods, such as chemical vapor deposition (CVD) or mechanical exfoliation, liquid-phase exfoliation (LPE) followed by self-assembling Langmuir–Blodgett (LB) technique deposition represents a simple and inexpensive route that enables obtaining the thin, transparent, and low-resistance films of high crystal quality and graphene flakes free of chemical modifications (Coleman 2013, Kim *et al.* 2013, Tomašević-Ilić *et al.* 2016, Szabó *et al.* 2021).

The light-sensitive bio-hybrid composites, among the future generation of materials, has been attracted much attention because light-matter interaction is fundamental not only in basic and applied research but also in advanced technology, where fast and efficient performance is a prerequisite, *e.g.*, in information, security, energy conversion, and sensor technology (Wraight and Clayton 1974, Xua *et al.* 2004, Tamiaki *et al.* 2006, Nagy *et al.* 2010, 2014; Cogdell *et al.* 2013, Hartmann *et al.* 2014, Szabó *et al.* 2015, Daliento *et al.* 2017, Hajdu *et al.* 2017, 2021; Ryu *et al.* 2018, Allen *et al.* 2022). Bio-hybrid composites, as the combination of carbon-based materials and light-sensitive biological molecules such as photosynthetic proteins, can be designed to convert light very efficiently into different kinds of energy forms within a tuneable time from femtoseconds to seconds and wavelength range from UV to IR, at the same time fulfilling another requirement that they are highly degradable into environmentally safe products.

Various photosynthetic materials, from light-sensitive pigments through macromolecules and molecular complexes to individual organisms, are already successfully combined with metal or semiconductor electrodes, as well as with carbon-based carrier matrices to benefit from the properties of both the biological and inorganic carriers. Photosynthetic reaction center proteins (pRC), which are known as 'nature's solar batteries' (Jones 2009), are the focus of numerous research aiming to create light-responsive low-power hybrid bio-optoelectronic devices (Tangorra *et al.* 2014, Csiki *et al.* 2018, Heifler *et al.* 2020, Altamura *et al.* 2021). In addition to the classical three-electrode electrochemical cells, typical architecture is an electrolyte-gated field-effect organic transistor arrangement in which redistribution of the photogenerated charges by the pRC drives photocurrent in suitable aqueous solution (Andronescu and Schuhmann 2017, Takshi *et al.* 2017, Zhang *et al*. 2017, Di Lauro *et al.* 2020).

It is already demonstrated that pRC isolated from the natural environment can preserve its photochemical/-physical activity to a large extent when dissolved in a water-based detergent micellar system, organic solvents (*e.g.*, hexane) (Tandori *et al.* 1991, Warncke and Dutton 1993) or even dried on inorganic carrier surfaces. It is known from the middle of the 1970s that pRCs keep their photoactivity when dried in chromatophores (the photosynthetic membrane in cells) on glass plates (Vermeglio and Clayton 1976, Clayton 1978). Purified pRCs also keep the photochemical/-physical activity when dried in gelatin films (Rafferty and Clayton 1979), in trehalose glasses (Palazzo *et al.* 2008), when bound to carbon nanotubes (CNTs), and dried on optical glass (Dorogi *et al.* 2006, Hajdu *et al.* 2011) or graphene (Szabó *et al.* 2021). CNTs can mimic the membrane environment and have a stabilization effect on the light-separated charges – the lifetime of the light-induced charge pair is increased, the redox species in the pRCs interact with the CNT (Dorogi *et al.* 2006), and the photochemical stability is kept for several months (Magyar *et al.* 2011). Exceptional stability and mechanical flexibility of the pRC-electrode system were reported where pRCs were directly immobilized on transparent graphene oxide (mRGO) electrodes (Zhang *et al.* 2017).

In the present work, we characterized dried bacterial photosynthetic reaction centers/graphene composite on SiO_2/Si wafer aiming to examine its photochemical/-physical activity as a light energy-converting system. The liquid-phase exfoliated graphene film was tested as a carrier in this configuration and the deposition of pRC onto its surface formed of closely packed graphene nanoflakes was performed by the drop-casting method. Different techniques, such as optical spectroscopy (Raman spectroscopy), microscopy techniques (scanning electron microscopy – SEM and atomic force microscopy – AFM), and electrical measurement based on light-induced change in $I_{source\text{-}drain}/U_{gate}$, were applied to investigate the properties of the complex after its drying. We demonstrated that films obtained using the LB technique from LPE graphene dispersion, have overlapping and edge-to-edge contact nanoflakes, providing the uniform large-area thin film suitable for the role of the carrier in the bio-hybrid complex for the optoelectronic devices.

Materials and methods

Reaction center purification: Reaction center protein was isolated from the intracytoplasmic membrane fraction of *Rhodobacter sphaeroides* 2.4.1 purple bacterial strain by detergent (LDAO, N,N-dimethyldodecylamine-N-oxide) solubilization and further purified by ammonium sulfate precipitation followed by (*DEAE Sephacell*) anion-exchange chromatography (Tandori *et al.* 1995). Both the primary (Q_A) and the secondary (Q_B) electron acceptor quinones were extracted according to Okamura *et al.* (1975). The sample was adjusted to about 60 μM pRC concentration, kept in a freezer at –77°C, and diluted to

the required concentration (*ca.* 10^{-9} M) to ensure monolayer coverage (Szabó *et al.* 2013, 2021) when it was used.

Preparation of graphene thin films: The graphene films were made at a water–air interface by Langmuir–Blodgett assembly (LBA) technique using liquid-phase exfoliated graphene, following the protocol described in earlier publications (Kim *et al.* 2013, Matković *et al.* 2016, Tomašević-Ilić *et al.* 2016). The commercial graphite powder (*Sigma Aldrich-332461*) was dissolved in N-methyl-2-pyrrolidone (NMP, *Sigma Aldrich-328634*) at an initial concentration of 18 mg ml^{-1}. After 14 h of sonication, in a low-power ultrasonic bath (*Bransonic CPXH Ultrasonic & Cleaning Bath*, 30 W), graphene dispersion was centrifuged at 3,000 rpm for 60 min using *Force 1624* microcentrifuge. Sonication time was optimised for obtaining the highest yield and quality of graphene nanoflakes with our ultrasound bath. We used the low-power bath, and we were adding the cool water every couple of hours, which kept the temperature in the bath close to the room temperature. By adding a small amount of graphene dispersion (0.3 ml) into the half-filled beaker of de-ionized (DI) water (electrical resistance of 18.2 MΩ) hydrophobic graphene nanosheets self-organize and form a close-packed thin film at the water–air interface. For transferring this film onto SiO_2/Si substrate (SiO_2 thickness of 80 ± 5 nm; Tomašević-Ilić *et al.* 2016) a simple automated dip-coater system (motorized pull-out sample holder) with vertical speed control allowed us to pull the substrate slowly through the interface and scoop the film without disturbing its integrity. After the transfer, the graphene film was left to dry in ambient conditions. To assess the integrity and morphology of our graphene samples, we used an atomic force microscope *N-Tegra Prima* (*NTMDT*, Russia) operating in a semi-contact mode and scanning electron microscopy (SEM). SEM images were taken at 15 kV acceleration voltage using a *Tescan MIRA3* field-emission gun (*Tescan*, Czech Republic). The statistics of the size of graphene nanoflakes was obtained using the SEM inbuilt software tools for selecting, outlining, and measuring their lateral size. For measuring the roughness and thickness profile in AFM images, we used the free *Gwyddion* software.

Preparing the pRC/graphene composite: After the graphene film has passed the quality control in morphology measurements, photosynthetic reaction centers, purified from *Rb. sphaeroides* 2.4.1 strain, were deposited on its surface by drop-casting. Following our earlier protocols (Kim *et al.* 2013, Matković *et al.* 2016, Tomašević-Ilić *et al.* 2016), pRC solution was dropped on the surface of graphene. The RC concentration was set to 1.25 nM, and the amount of LDAO was reduced to 0.006%, well below the c.m.c. (0.01%) by dialysis, and 5 µL pRC solution was dried at room temperature under an air stream to ensure approximately single-layer pRC coverage (Szabó *et al.* 2013, 2021) in a 2-mm diameter spot. No specific attempt was made for oriented binding of the RC to graphene in these experiments; this can be the aim of the following investigations. However, by using CNT and pRCs in our earlier investigations, we learned that hydrophobic–hydrophobic interactions play probably the major role (the main thermodynamic driving force) of the stabilization (Dorogi *et al.* 2006). The probably random orientation of the pRC is determined by the hydrophobic interaction between the graphene flakes and the membrane-spanning part of the pRC, maybe, with the involvement of π-stacking, without specific selection of the e^--donor or the -acceptor side of the protein.

Raman microscopy for spectroscopy: Raman spectra were obtained using the *NTegra Spectra P9* (*NT-MDT Spectrum Instruments*, Limerick, Ireland) controller and microscope, having a 100× objective, under ambient air conditions at room temperature. For the excitation, a 473-nm wavelength diode laser was used, while for spectral decomposition, a 300 groves mm^{-1} grating covering the range of 180–3,500 cm^{-1}. Before experiments, the system was calibrated to the first peak of a silicon surface at 520.5 cm^{-1}. Individual spectra were collected with a step size of 500 nm covering a total area of 40 µm × 20 µm resulting in 3,200 spectra in total. After all spectra were averaged, the background was removed by fitting the lowest count values with a 7th-order polynomial (Szőke *et al.* 2020).

Measuring current-voltage characteristics: Before the measurement, connecting electrodes were fixed by water-based carbon paste (*SUPELCO*) to Si (gate) and graphene (source and drain). Light-induced changes were measured by exciting the sample with a continuous wave laser diode (*CWDL*, 2 W, 808 nm, *Roithner*). The signal was detected by a *Keithley 2700* multimeter (*Tektronix Inc.*, USA) with a 6.5-digit resolution (Magyar *et al.* 2011, Szabó *et al.* 2013, 2021). Based on our earlier experiments (Szabó *et al.* 2021), the intensity of the exciting CWDL light was set to the maximum value of the linear increase in the current signal, and grey filters (reached around 1 mW cm^{-2} of light intensity) were used to minimize the probability of multiple excitations of the pRC. The measurements were controlled, and the data were collected and analysed using the self-developed *LabVIEW* software. The experimental arrangement for measuring light-induced changes in the electric properties of the graphene/pRC bio-hybrid is depicted in Fig. 1.

Results and discussion

Structural characterizations: Information about the structural characteristic of the film and its morphology was obtained using SEM (Fig. 2). It can be noticed in Fig. 2*A* that graphene flakes completely cover the substrate forming the film through overlapping and positioning side-by-side. For SEM image analysis, the nanoflakes were selected using the inbuilt instrument software, and their size was measured with appropriate software tools. The arrangement of the graphene flakes implies the mesoporous structure of the film. Fig. 2*B* presents histograms of the lateral sizes of graphene flakes, indicating that their average diameter was 130 ± 10 nm.

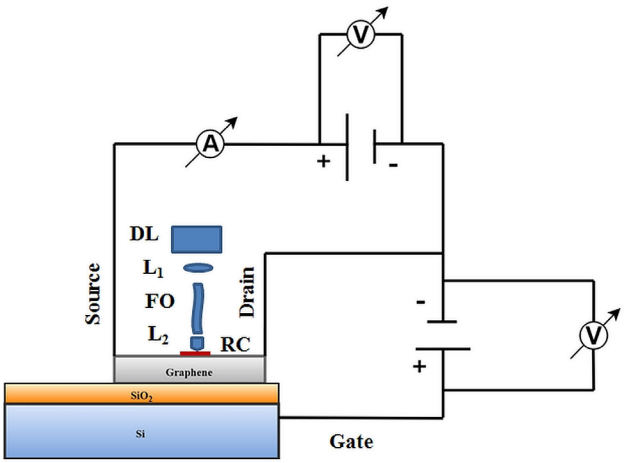

Fig. 1. Schematic representation of the experimental arrangement. CWDL – diode laser; L_1 and L_2 – lenses; FO – fiber optics; RC – reaction centre.

Further analysis of the graphene film surface was performed by AFM. The AFM topographic images (Fig. 3) confirmed good surface coverage of the SiO_2/Si substrate by overlapping graphene nanoflakes. Using the statistical analysis with the *Gwyddion* software enabled us to estimate the average roughness of the film in the order of 10 nm. The overlap of individual graphene nanoflakes in the film prevented the exact measurement of their thickness by AFM. However, it has been established in our previous work (Matković *et al*. 2016) that the graphene flakes obtained using our exfoliation protocol were composed of a few layers, comparable to the size of the pRC particle.

Considering that the pRC water solution also contains the surfactant (although well below the c.m.c., which is sufficiently enough to keep the pRC in suspension) that stabilizes the protein particles and prevents their agglomeration, we assumed that the drop-casted pRC would likely be randomly distributed over the drop area and not accumulate anywhere in particular. Therefore, we can consider our composite structure to be close to a monolayer of pRC on graphene, as in our earlier experiments (Szabó *et al.* 2013, 2021).

To confirm the pRC adsorption on the graphene film, the sample coverage was analysed by Raman microscopy in the range of 180–3,500 cm^{-1} where the characteristic peaks of Si, graphene, pRC carotenoids, and NH- and saturated CH-bands can be visualized (Adar 2022). As a reference, Raman spectra of multilayer pRCs deposited onto SiO_2/Si were recorded. Fig. 4 shows that the characteristic peaks of Si/SiO_2, graphene, and the numbers of the pRC peak can be clearly identified and coincide well with the ones reported already in the literature for the pRC (Robert 1990) and for Si/SiO_2/graphene substrates (Hrubý *et al.* 2020). At 473-nm laser excitation preferentially, the carotenoids bound to pRC are excited and show characteristic resonance peaks. When RCs are bound to graphene film, probably, due to large overlap with graphene, the carotenoid peaks are reduced considerably, however, in the range of CH-NH bands of the spectrum, the pRC binding is indicated. The positions and modifications of the peaks due to different pRC conditions (substrate binding, environment, light–dark, *etc*.) are a matter of further investigation.

Electric current measurements: The thin graphene film transferred onto the SiO_2/Si substrate (Si is n-type of semiconductor) shows the diode-like I/V characteristics due to the good contact at the interface (Fig. 1). Fig. 5 shows that the current in the dark equilibrium can clearly be distinguished in the negative and the positive directions. When the device is illuminated by light, current flow opens in the positive U_G (Fig. 5) without affecting the current in the negative U_G (Fig. 5) with or without the pRC coverage.

The asymmetric light response with the gate voltage is better demonstrated when the 'light minus dark' drain-source (I_{DS}) current is plotted *vs*. the gate voltage (U_G, Fig. 6). In this representation, the signal is compensated with any (electric and/or thermal) effect accompanying the light excitation in the Si, SiO_2, and graphene phases and/or at the interfaces. Light-induced changes in the I_{DS} can be seen only in the positive U_G range and are enhanced significantly when graphene is functionalized with the pRCs. The change in the drain-source current does not show dependence on the drain-source voltage (U_{DS}) (in the investigated range, 0–1,000 mV, at least), however, is highly sensitive to U_G.

There are multiple effects of the excitation of this layered structure by light in the near-infrared range (the excitation wavelength in our case was 808 nm).

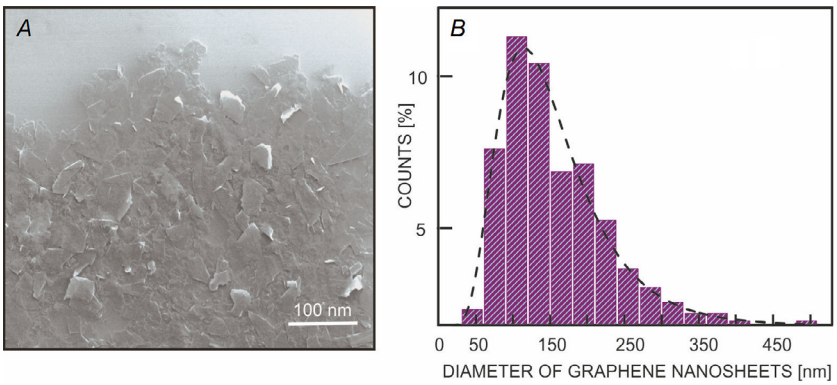

Fig. 2. (*A*) SEM image of graphene film on SiO_2/Si wafer, (*B*) histograms of graphene nanosheet diameter obtained from five 2 × 2 μm^2 SEM images (~1,400 flakes). *The black dashed line* corresponds to the log-normal fit.

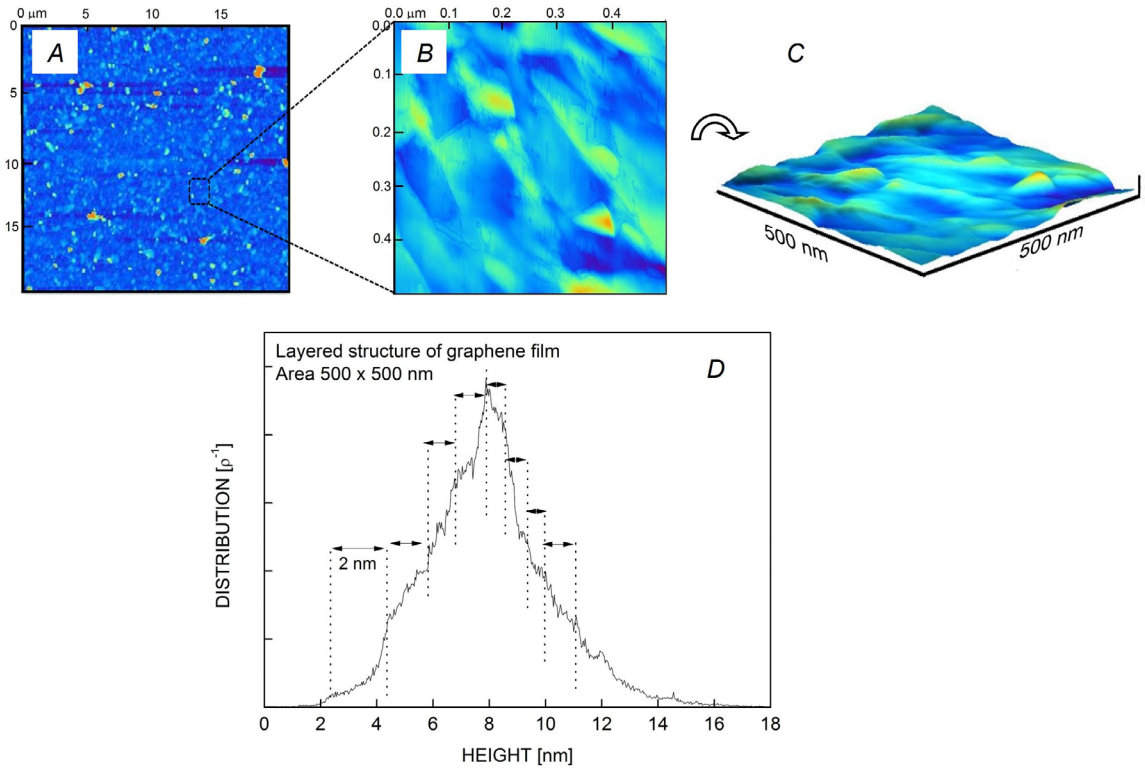

Fig. 3. AFM mapping of graphene thin films on the SiO2/Si substrate (colours represent the virtual gradient in height): top images – graphene flakes are fully covering the substrate (20 × 20 μm scan), with mean height distribution of 36 ± 2 nm, and roughness parameter (root mean square, RMS) of 13 ± 5 nm, detail of a large scan – height distribution shows the layered structure and overlap of graphene flakes (500 × 500 nm scan), with the thickness ranging from less than 1 nm to several nanometres.

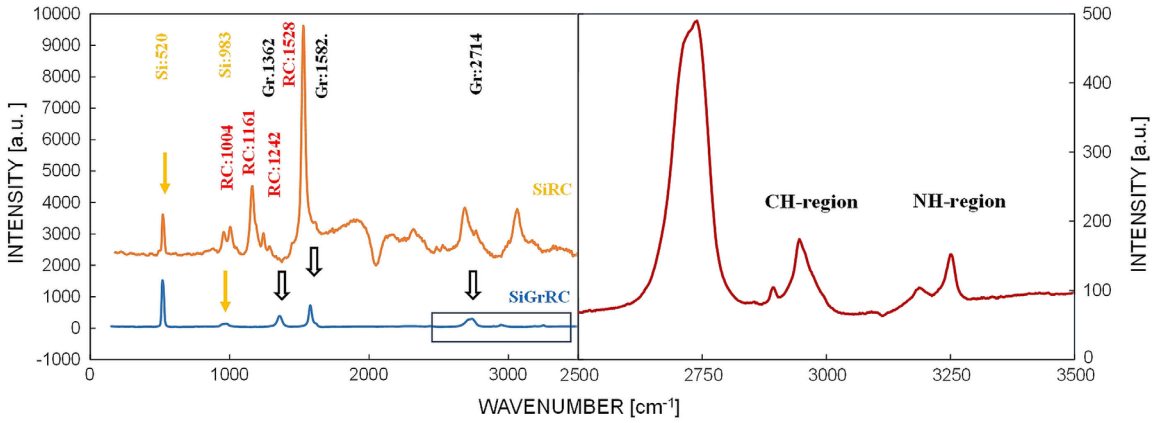

Fig. 4. *Left*: Raman intensity of RC thin film combined on graphene/SiO_2/Si substrate (SiGrRC) and RC deposited on SiO_2/Si (SiRC) in the range of 180–3,700 cm^{-1}. The characteristic peaks of SiO_2/Si, graphene, and reaction centres are indicated. *Solid and open arrows* indicate positions of SiO_2/Si and graphene, respectively. *The open box* indicates the range of the spectrum indicated in the right figure. *Right*: Raman intensity of RC thin film combined on graphene/SiO_2/Si substrate in the CH-NH range of the spectrum. The spectral range is depicted from the range indicated in the open box in the left figure.

Although graphene film does not have a plasmonic excitation at this wavelength, thermal dissipation of the absorbed photon energy is very likely an alternative reason for the change in I/V. In addition, due to the relatively large transparency of the graphene film, light can induce an electronic excitation of the Si bulk, as well as the conductivity change at the interfaces of Si/SiO_2/graphene. Structural and functional conditions of the pRC deposition were optimized to reduce the possible artifacts (*e.g.*, due to integrity of the protein structure, overexcitation of the photochemistry/-physics of the pRC, possible effects of the detergent on the RC–substrate interaction; *see* 'Materials and methods, Preparing the pRC/graphene composite') in the light-induced current changes.

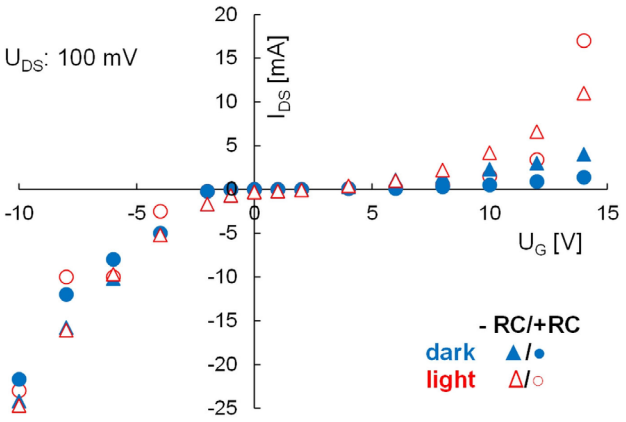

Fig. 5. Typical transient of the drain-source current (I_{DS}) *vs*. gate voltage (U_G) in graphene on silicon oxide with or without RCs in the dark or under light excitation, as indicated. Measurement was carried out with drain-source voltage (U_{DS}) fixed at 100 mV.

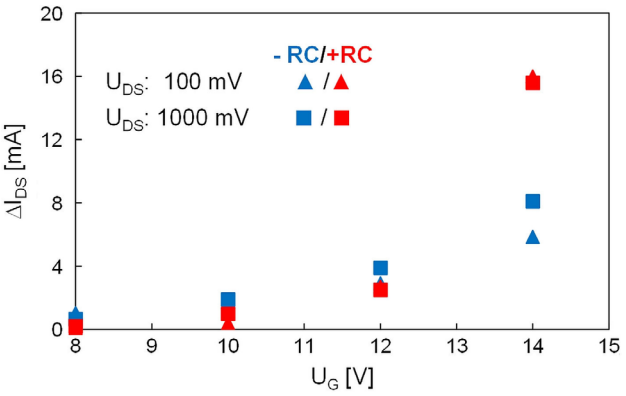

Fig. 6. Light-minus-dark drain-source current (ΔI_{DS}) of the graphene with or without the RC as a function of the gate voltage (U_G) under two drain-source voltage values (U_{DS} = 100 mV and 1,000 mV, as indicated).

Because of the effects, which are 'non-specific' to the charge transfer in pRCs (possible artifact-like signals, temperature effect, events in the bulk phase of Si, SiO_2, graphene or at the interfaces, *etc.*), the absolute current values show some variations, so that Fig. 5 shows results of individual measurements with typical characteristics. However, these non-specific 'side effects' can be subtracted, the results of individual samples can be compensated, and the light-induced current enhancement is better visualized when light-minus-dark transients are represented.

It must be noted that the measurements were carried out under conditions when pRCs were dried without reconstituting the donor and acceptor sides by artificial external e^- donors or acceptors. Under these conditions, the pRC is not capable of performing multiple turnovers of the photocycle, only single charge separation followed by charge recombination occurs. In pRCs purified from *Rb. sphaeroides* 2.4.1, the e^--acceptor quinones were completely depleted, PBPheo → P^+BPheo^- charge separation occurred in a ps-time scale after excitation by light followed by recombination in about tens of nanoseconds (P^+BPheo^- → PBPheo) (Nagy *et al.* 2015). Here, P and P^+, BPheo, and $BPheo^-$ are the reduced and oxidized primary e^--donor and bacteriopheophytin, respectively. There is a large number of reports in the literature about direct electronic interaction between redox centers of the pRC and carrier matrices (*e.g.*, electrode surfaces in electrochemical cells for attempting photovoltaic or biosensor applications). In these reported experiments, the full photocycle of the pRC is fulfilled, usually in traditional electrochemical cells (*cf.* 'Introduction'). At the present state of our experiments, we do not have direct evidence for the contribution either of charge transfer between the pRC and graphene or of the effect of the electric field. Because the electron transfer through the pRC is blocked, the redox transient of the pRC probably does not contribute significantly to the charge density in the graphene layer, however, the interaction between the electric fields can be accounted for.

Conclusions: This is the first report to show that the dried bacterial photosynthetic reaction centers/graphene composite on SiO_2/Si performs a photochemical/-physical activity and this activity is in interaction with the graphene carrier matrix. The current through the possible Si/SiO_2/graphene/pRC junction is sensitive to light, due to the contribution from the light-activated pRC to the applied gate and DS voltages. Our data provide useful information for the future direction of creating simple and efficient light-responsive low-power hybrid bio-optoelectronic organic devices. One reasonable improvement of dry pRC/graphene devices could be achieved by providing specific donor–acceptor sites on graphene for pRCs to bind at a specific orientation. A specific pattern and density of these sites will also provide more uniform and controlled adsorption of a larger amount of pRC, which in turn will improve their efficiency as an electric power source and/or specific optoelectronic devices. These experiments can also be done using specifically modified RCs in which the light-induced turnover rate and the spectral sensitivity can be modulated in a wide range in future experiments.

References

Adar F.: Interpretation of Raman spectrum of proteins. – Spectroscopy **37**: 9-13, 2022.

Allen J.P., Chamberlain K.D., Olson T.L., Williams J.C.: A bound iron porphyrin is redox active in hybrid bacterial reaction centers modified to possess a four-helix bundle domain. – Photoch. Photobio. Sci. **21**: 91-99, 2022.

Altamura E., Albanese P., Marotta R., Mavelli F.: Chromatophores efficiently promote light-driven ATP synthesis and DNA transcription inside hybrid multicompartment artificial cells. – PNAS **118**: e2012170118, 2021.

Andronescu C., Schuhmann W.: Graphene-based field effect transistors as biosensors. – Curr. Opin. Electrochem. **3**: 11-17, 2017.

Blake P., Brimicombe P.D., Nair R.R. *et al.*: Graphene-based liquid crystal device. – Nano Lett. **8**: 1704-1708, 2008.

Clayton R.K.: Effects of dehydration on reaction centers from *Rhodopseudomonas sphaeroides*. – BBA-Bioenergetics **504**: 255-264, 1978.

Cogdell R.J., Gardiner A.T., Molina P.I., Cronin L.: The use and misuse of photosynthesis in the quest for novel methods to harness solar energy to make fuel. – Philos. T. Roy. Soc. B **371**: 20110603, 2013.

Coleman J.N.: Liquid exfoliation of defect-free graphene. – Acc. Chem. Res. **46**: 14-22, 2013.

Csiki R., Drieschner S., Lyuleeva A. *et al.*: Photocurrent generation of biohybrid systems based on bacterial reaction centers and graphene electrodes. – Diam. Relat. Mater. **89**: 286-292, 2018.

Daliento D., Chouder A., Guerriero P. *et al.*: Monitoring, diagnosis, and power forecasting for photovoltaic fields: a review. – Int. J. Photoenergy **2017**: 1356851, 2017.

Darder M., Aranda P., Ruiz-Hitzky E.: Bionanocomposites: a new concept of ecological, bioinspired and functional hybrid materials. – Adv. Mater. **19**: 1309-1319, 2007.

Di Lauro M., la Gatta S., Bortolotti C.A. *et al.*: A bacterial photosynthetic enzymatic unit modulating organic transistors with light. – Adv. Electron. Mater. **6**: 1900888, 2020.

Dorogi M., Bálint Z., Mikó C. *et al.*: Stabilization effect of single-walled carbon nanotubes on the functioning of photosynthetic reaction centers. – J. Phys. Chem. B **110**: 21473-21479, 2006.

Geim A.K.: Graphene: status and prospects. – Science **324**: 1530-1534, 2009.

Geim A.K., Novoselov K.S.: The rise of graphene. – Nat. Mater. **6**: 183-191, 2007.

Giraldo J.P., Landry M.P., Faltermeier S.M. *et al.*: Plant nanobionics approach to augment photosynthesis and biochemical sensing. – Nat. Mater. **13**: 400-408, 2014.

Hajdu K., Balderas-Valadez R.F., Carlino A. *et al.*: Porous silicon pillar structures/photosynthetic reaction centre protein hybrid for bioelectronic applications. – Photoch. Photobio. Sci. **21**: 13-22, 2021.

Hajdu K., Szabó T., Magyar M. *et al.*: Photosynthetic reaction center protein in nanostructures. – Phys. Status Solidi B **248**: 2700-2703, 2011.

Hajdu K., Szabó T., Sarrai A.E. *et al.*: Functional nanohybrid materials from photosynthetic reaction center proteins. – Int. J. Photoenergy **2017**: 9128291, 2017.

Hartmann V., Kothe T., Pöler S. *et al.*: Redox hydrogels with adjusted redox potential for improved efficiency in Z-scheme inspired biophotovoltaic cells. – Phys. Chem. Chem. Phys. **16**: 11936-11941, 2014.

Heifler O., Carmeli C., Carmeli I.: Chemical tagging of membrane proteins enables oriented binding on solid surfaces. – Langmuir **36**: 4556-4562, 2020.

Hrubý J., Vavrečková Š., Masaryk L. *et al.*: Deposition of tetracoordinate Co(II) complex with chalcone ligands on graphene. – Molecules **25**: 5021, 2020.

Jones M.R.: The petite purple photosynthetic powerpack. – Biochem. Soc. T. **37**: 400-407, 2009.

Kim H., Mattevi C., Kim H.J. *et al.*: Optoelectronic properties of graphene thin films deposited by a Langmuir–Blodgett assembly. – Nanoscale **5**: 12365-12374, 2013.

Kim K.S., Zhao Y., Jang H. *et al.*: Large-scale pattern growth of graphene films for stretchable transparent electrodes. – Nature **457**: 706-710, 2009.

Li X., Zhu Y., Cai W. *et al.*: Transfer of large-area graphene films for high-performance transparent conductive electrodes. – Nano Lett. **9**: 4359-4363, 2009.

Luka G., Ahmadi A., Najjaran H. *et al.*: Microfluidics integrated biosensors: a leading technology towards lab-on-a-chip and sensing applications. – Sensors-Basel **15**: 30011-30031, 2015.

Magyar M., Hajdu K. Szabó T. *et al.*: Long term stabilization of reaction center protein photochemistry by carbon nanotubes. – Phys. Status Solidi B **248**: 2454-2457, 2011.

Magyar M., Hajdu K., Szabó T. *et al.*: Sensing hydrogen peroxide by carbon nanotube/horse radish peroxidase bio-nanocomposite. – Phys. Status Solidi B **250**: 2559-2563, 2013.

Magyar M., Rinyu L., Janovics R. *et al.*: Real-time sensing of hydrogen peroxide by ITO/MWCNT/horseradish peroxidase enzyme electrode. – J. Nanomater. **2016**: 2437873, 2016.

Matković A., Milošević I., Milićević M. *et al.*: Enhanced sheet conductivity of Langmuir–Blodgett assembled graphene thin films by chemical doping. – 2D Materials **3**: 015002, 2016.

Nagy L., Hajdu K., Fisher B. *et al.*: Photosynthetic reaction centres – from basic research to application possibilities. – Not. Sci. Biol. **2**: 7-13, 2010.

Nagy L., Kiss V., Brumfeld V. *et al.*: Thermal effects and structural changes of photosynthetic reaction centers characterized by wide frequency band hydrophone: Effects of carotenoids and terbutryn. – Photochem. Photobiol. **91**: 1368-1375, 2015.

Nagy L., Magyar M.: No alternatives to photosynthesis: from molecules to nanostructures. – In: Jeschke P., Starikov E.B. (ed.): Agricultural Biocatalysis: Theoretical Studies and Photosynthesis Aspects. Pp. 210-247. Jenny Stanford Publishing, New York 2022.

Nagy L., Magyar M., Szabó T. *et al.*: Photosynthetic machineries in nano-systems. – Curr. Protein Pept. Sci. **15**: 363-373, 2014.

Okamura M.Y., Isaacson R.A., Feher G.: Primary acceptor in bacterial photosynthesis: obligatory role of ubiquinone in photoactive reaction centers of *Rhodopseudomonas sphaeroides*. – PNAS **72**: 3491-3495, 1975.

Palazzo G., Francia F., Mallardi A. *et al.*: Water activity regulates the Q_A^- to Q_B electron transfer in photosynthetic reaction centers from *Rhodobacter sphaeroides*. – J. Am. Chem. Soc. **130**: 9353-9363, 2008.

Rafferty C.N., Clayton R.K.: Linear dichroism and the orientation of reaction centers of Rhodopseudomonas sphaeroides in dried gelatin films. – BBA-Bioenergetics **545**: 106-121, 1979.

Robert B.: Resonance Raman studies of bacterial reaction centers. – BBA-Bioenergetics **1017**: 99-111, 1990.

Ryu D.H., Kim Y.J., Kim S.I. *et al.*: Thylakoid-deposited micro-pillar electrodes for enhanced direct extraction of photosynthetic electrons. – Nanomaterials **8**: 189, 2018.

Shoseyov O., Levy I.: NanoBioTechnology: BioInspired Devices and Materials of the Future. Pp. 485. Humana Press, Totowa 2008.

Szabó T., Bencsik G., Magyar M. *et al.*: Photosynthetic reaction centers/ITO hybrid nanostructure. – Mater. Sci. Eng. C **33**: 769-773, 2013.

Szabó T., Csekő R., Hajdu K. *et al.*: Sensing photosynthetic herbicides in an electrochemical flow cell. – Photosynth. Res. **132**: 127-134, 2017.

Szabó T., Magyar M., Hajdu K. *et al.*: Structural and functional hierarchy in photosynthetic energy conversion – from molecules to nanostructures. – Nanoscale Res. Lett. **10**: 458, 2015.

Szabó T., Panajotović R., Vujin J. *et al.*: Photosynthetic reaction-center/graphene biohybrid for optoelectronics. – J. Nanosci. Nanotechnol. **21**: 2342-2350, 2021.

Szőke Á.F., Szabó G.S., Hórvölgyi Z. *et al.*: Accumulation of 2-acetylamino-5-mercapto-1,3,4-thiadiazole in chitosan coatings for improved anticorrosive effect on zinc. – Int. J. Biol. Macromol. **142**: 423-431, 2020.

Takshi A., Yaghoubi H., Wang J. *et al.*: Electrochemical field-effect transistor utilization to study the coupling success rate of photosynthetic protein complexes to cytochrome *c*. – Biosensors **7**: 16, 2017.

Tamiaki H., Nishihara K., Shibata R.: Synthesis of self-aggregative zinc chlorophylls possessing polymerizable esters as a stable

model compound for main light-harvesting antennas of green photosynthetic bacteria. – Int. J. Photoenergy **2006**: 090989, 2006.

Tandori J., Nagy L., Maróti P.: Semiquinone oscillation as a probe of quinone/herbicide binding in bacterial reaction centers. – Photosynthetica **25**: 159-166, 1991.

Tandori J., Nagy L., Puskás A. *et al.*: The Ile^{L229} → Met mutation impairs the quinone binding to the Q_B-pocket in reaction centers of *Rhodobacter sphaeroides*. – Photosynth. Res. **45**: 135-146, 1995.

Tangorra R.R., Antonucci A., Milano F. *et al.*: Photoactive film by covalent immobilization of a bacterial photosynthetic protein on reduced graphene oxide surface. – MRS Online Proceedings Library **1717**: 12-18, 2014.

Tomašević-Ilić T., Pešić J., Milošević I. *et al.*: Transparent and conductive films from liquid phase exfoliated graphene. – Opt. Quant. Electron. **48**: 319, 2016.

Vermeglio A., Clayton R.K.: Orientation of chromophores in reaction centers of *Rhodopseudomonas sphaeroides*. Evidence for two absorption bands of the dimeric primary electron donor. – BBA-Bioenergetics **449**: 500-515, 1976.

Wang X., Zhi L., Müllen K.: Transparent, conductive graphene electrodes for dye-sensitized solar cells. – Nano Lett. **8**: 323-327, 2008.

Warncke K., Dutton P.L.: Experimental resolution of the free energies of aqueous solvation contributions to ligand-protein binding: quinone-Q_A site interactions in the photosynthetic reaction center protein. – PNAS **90**: 2920-2924, 1993.

Wraight C.A., Clayton R.K.: The absolute quantum efficiency of bacteriochlorophyll photooxidation in reaction centres of *Rhodopseudomonas sphaeroides*. – BBA-Bioenergetics **333**: 246-260, 1974.

Xua J., Bhattacharya P., Váró G.: Monolithically integrated bacteriorhodopsin/semiconductor opto-electronic integrated circuit for a bio-photoreceiver. – Biosens. Bioelectron. **19**: 885-892, 2004.

Zhang H., Carey A.-M., Jeon K.-W. *et al.*: A highly stable and scalable photosynthetic reaction center–graphene hybrid electrode system for biomimetic solar energy transduction. – J. Mater. Chem. A **5**: 6038-6041, 2017.